Sensors and Actuators B 134 (2008) 981–987

Contents lists available at ScienceDirect

Sensors and Actuators B: Chemical

journal homepage: www.elsevier.com/locate/snb

A thin-film transistor based acetylcholine sensor using self-assembled carbon nanotubes and SiO_2 nanoparticles

Wei Xue[a,b], Tianhong Cui[a,*]

[a] Department of Mechanical Engineering, University of Minnesota, Twin Cities, 111 Church Street SE, Minneapolis, MN 55455, USA
[b] Department of Mechanical Engineering, Washington State University, Vancouver, WA 98686, USA

ARTICLE INFO

Article history:
Received 22 April 2008
Received in revised form 2 July 2008
Accepted 3 July 2008
Available online 17 July 2008

Keywords:
Single-walled carbon nanotube (SWNT)
Thin-film transistor (TFT)
Ion-sensitive field-effect transistor (ISFET)
Acetylcholine sensor
Layer-by-layer (LbL) self-assembly

ABSTRACT

A high sensitivity acetylcholine (ACh) sensor is developed using a nanomaterial-based thin-film transistor. The device fabrication combines the "bottom-up" layer-by-layer self-assembly and the "top-down" microfabrication techniques. The transistor uses a self-assembled single-walled carbon nanotube (SWNT) multilayer as the semiconducting film. Silicon dioxide (SiO_2) nanoparticles are deposited on the substrate as the dielectric material. Acetylcholinesterase (AChE) enzyme molecules are immobilized on the surface as the sensing film, which can induce the ACh hydrolysis reaction and release hydrogen ions to the solution. Because all the assembly steps of the multilayer films are done in solutions at room temperature, the fabrication complexity and the process cost are dramatically reduced. The transistor-based sensor demonstrates high sensitivity for ACh sensing and shows a good linearity in the high ACh concentration range. The sensitivity, resolution, and response time of the sensor are measured as 378.2 μA/decade, 10 nM, and 15 s, respectively. This work presents a promising technique to develop disposable and high-sensitivity biosensors for a wide range of applications.

1. Introduction

Acetylcholine (ACh) is one of the most important neurotransmitters in human nervous systems. It is involved in many nervous activities including learning, attention, memory, and muscle contraction. The dysfunctional ACh regulation in the brain causes a number of neuropsychiatric disorders such as Parkinson disease, Alzheimer disease, and myasthenia gravis. Therefore, there has been growing interest in the development of accurate sensing methods to measure ACh concentration [1–3]. High-performance liquid chromatography (HPLC) method on microdialysis samples is a widely used technique for ACh measurement [4]. It is a high-resolution approach but the system setup is very expensive. A promising alternative approach is to use microscale devices because of their low cost and miniaturized size. Most microsensors use immobilized acetylcholinesterase (AChE) enzyme as the sensing material. The measurement of the ACh concentration is based on the hydrolysis process of ACh catalyzed by the AChE. The AChE-based microsensors have also been used to detect AChE inhibitors such as pesticides [5]. Common microsensors that have been developed for ACh sensing include amperometric devices [6], potentiometric electrodes [7], luminescent detectors [8], and ion-sensitive field-effect transistors (ISFETs) [9]. Among these devices, ISFET biosensor is an effective technique and provides a number of advantages: low workload on pre-sampling and post-analysis; high compatibility with the current microfabrication techniques; and easy integration with control circuits. Furthermore, the ISFET biosensors are standalone devices; they are robust and can operate in harsh conditions with wide temperature and pH ranges [10,11]. It is expected that the ISFET-based devices will continue to provide high-performance sensors and systems in the future.

However, most reported ISFET sensors are fabricated on bulk silicon (Si) substrates because the basic ISFET design evolves from the traditional metal-oxide-semiconductor field-effect transistor (MOSFET) structure. Even though these ISFETs demonstrate higher performance and wider applicability than most electrochemical sensors, their sensitivities are restricted by the planar structures: the accumulation or depletion of charge carriers only occurs in the surface region of the device. In contrast, the design and development of novel field-effect sensors using nanomaterials, especially carbon nanotubes and nanowires, provide an effective approach to overcome the limitations of the Si planar structures because of the scale and morphology of the nanomaterials [12]. Nanomaterial-based electronic devices have proven to be a powerful class of high-performance sensors.

Recently, we reported a single-walled carbon nanotube (SWNT) thin-film biosensor [13]. It demonstrates a high resolution, defined

* Corresponding author. Tel.: +1 612 626-1636; fax: +1 612 625-6069.
E-mail address: tcui@me.umn.edu (T. Cui).

0925-4005/$ – see front matter © 2008 Elsevier B.V. All rights reserved.
doi:10.1016/j.snb.2008.07.008

as the lowest measurable chemical concentration, of 100 pM for ACh sensing. The two-terminal resistor-like structure simplifies the fabrication and measurement procedures. However, the current shift range is small; the characterized sensitivity of the sensor is 7.2 μA/decade. Our group has also developed ISFET-based ACh sensors using novel materials. Y. Liu et al investigated the ISFET technology by using low-cost materials including polyaniline (PANI) and indium oxide (In_2O_3) nanoparticles [14,15]. The ISFET sensors demonstrate promising results for ACh sensing. However, these materials have low conductivities, which restrict the sensitivities of the fabricated sensors. The measured sensitivities for the PANI and In_2O_3 nanoparticles ISFETs are 1.4 and 12.4 μA/decade, respectively.

In order to further investigate the potential of nanomaterial-based microsensors, we modify the device design and develop a high-sensitivity ISFET ACh sensor using SWNTs and silicon dioxide (SiO_2) nanoparticles. The sensor is based on an SWNT thin-film transistor (TFT) structure. The SWNTs are layer-by-layer (LbL) self-assembled on the Si substrate as the semiconducting film; SiO_2 nanoparticles are coated as the dielectric film; and AChE enzyme molecules are immobilized on the surface as the sensing film. Compared with the PANI and In_2O_3 nanoparticles, the SWNTs have a much higher conductivity, which provides the ISFET with an enhanced working current. The current variation caused by the target analytes with difference concentrations is increased as well. The SWNT ISFET demonstrates a high sensitivity of 378.2 μA/decade. In addition, the sensor shows promising performance for ACh sensing in terms of resolution and response time. The structure, fabrication, and characterization of the SWNT ISFET sensor are described and discussed in this paper.

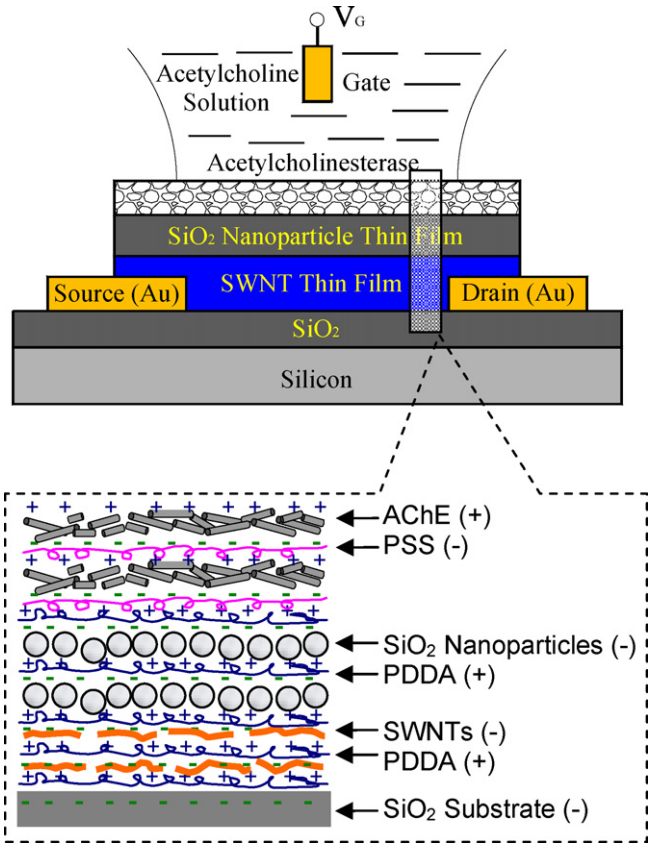

Fig. 1. Schematic illustration of an SWNT thin-film transistor based ACh sensor. The enlarged area demonstrates the model structure of the layer-by-layer self-assembled multilayers.

2. Experiments

All the chemicals used in the experiments were commercially available. They were diluted with deionized water to obtain optimum concentrations. The pristine SWNTs (powder, 1.1 nm in diameter, 50 μm in length, density of 2.1 g/cm^3, purity >90%, purchased from Chengdu Organic Chemical Co. Ltd.) were treated with a mixture of 1:3 HNO_3:H_2SO_4 acids at 110 °C for 45 min to increase the solubility in water. The final concentration of the SWNT dispersion was 1 mg/ml. The SiO_2 nanoparticle dispersion (colloidal silica, 45 nm in diameter, from Nissan Chemical Industries Ltd.) was diluted to 40 mg/ml. AChE and ACh were purchased from Sigma-Aldrich. The AChE was diluted to 10 μg/ml. NaCl (0.1 mM) was added to the AChE solution for ionic strength enhancement. The ACh was diluted with deionized water to various concentrations, from 1 pM to 10 mM, for measurements. The SWNTs and SiO_2 nanoparticles are negatively charged materials and the AChE is a positively charged enzyme. Two polyelectrolytes (both from Sigma-Aldrich), poly(dimethyldiallylammonium chloride) (PDDA, polycation, molecular weight 200,000–350,000, concentration 15 mg/ml) and poly(sodium 4-styrenesulfonate) (PSS, polyanion, molecular weight 70,000, concentration 3 mg/ml), were used as the electrostatic "glue" in the LbL self-assembly process to form stable and strong multilayer films. More detailed information about the material preparation can be found in our previous reports [13,16].

The device design of the SWNT ISFET was based on our previously reported high-mobility thin-film transistor [17], as shown in Fig. 1. The device was fabricated on a Si/SiO_2 substrate. Au was used as the source/drain electrode material. The gate electrode was an Ag/AgCl probe instead of a metal layer directly deposited on the device surface. Three multilayer films were coated on the substrate: SWNTs, SiO_2 nanoparticles, and AChE enzyme molecules were used as the semiconducting, dielectric, and sensing materials, respectively. The immobilized AChE enzyme can hydrolyze ACh into choline and acetic acid, and release hydrogen ions (H^+) to the solution.

The device fabrication combined the "bottom-up" LbL self-assembly and the "top-down" microfabrication techniques. The fabrication procedure of the ISFET started with electron-beam evaporation of Cr/Au (100/200 nm) layers on a Si/SiO_2 substrate. The metal layers were patterned as electrode pads. The distance between the pads, or the channel length of the semiconducting film, was 5 μm. The channel width was 1 mm. The substrate was then alternatively immersed in aqueous solutions with controlled time periods for the LbL self-assembly process. First, a $(PDDA/PSS)_2$ multilayer was deposited on the substrate as the precursor layer, which can enhance the subsequent adsorption of SWNTs and nanoparticles. The coating sequence of the precursor layer was [PDDA (10 min) + PSS (10 min)]$_2$. Next, three multilayer films, in a chronological sequence of $(PDDA/SWNT)_5$, $(PDDA/SiO_2$ nanoparticles$)_6$, and $(PSS/AChE)_3$ multilayers, were self-assembled on the substrate. To obtain uniformly deposited films with good surface coverage, the assembly processes of the three materials were monitored using a quartz crystal microbalance (QCM) [18]. The assembly time periods for SWNTs, SiO_2 nanoparticles, and AChE molecules were 15, 4, and 15 min, respectively. The QCM characterization showed that the effective thicknesses of the three multilayers were 38, 180, and 27.6 nm, respectively. As a result, the film on the surface was composed of $(PDDA/PSS)_2 + (PDDA/SWNT)_5 + (PDDA/SiO_2)_6 + (PDDA)_1 + (PSS/AChE)_3$. Before the LbL self-assembly process, a photoresist layer was patterned as sacrificial structures to protect the electrode pads. The sacrificial photoresist was removed by acetone using the lift-off technique

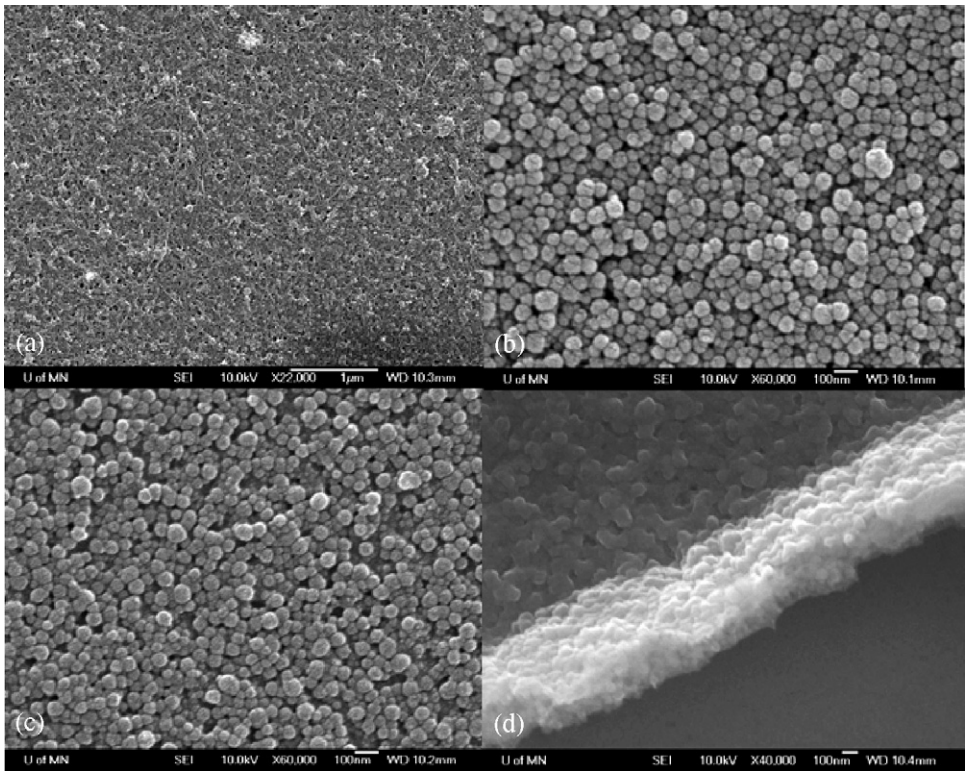

Fig. 2. SEM images of self-assembled (a) SWNTs, (b) SiO_2 nanoparticles, and (c) AChE enzyme molecules. The AChE molecules are grown on the surface of the nanoparticle film. (d) Cross-sectional view of the $(PDDA/SWNT)_5(PDDA/SiO_2)_6$ multilayer film.

after the self-assembly process. The electrode pads were therefore exposed.

The self-assembled multilayers were inspected by a scanning electron microscope (SEM). Five (PDDA/SWNT) bilayers completely cover the substrate and form a dense network, as shown in Fig. 2(a). The SWNTs are tangled together and randomly deposited on the surface. Fig. 2(b) shows the top view of the $(PDDA/SiO_2)_6$ multilayer film. Fig. 2(c) illustrates the same sample after a $(PDDA)(PSS/AChE)_3$ multilayer film is assembled on the surface. The SiO_2 nanoparticles are still visible in this image. The reason is that the thickness of the AChE film is only 27.6 nm, which is much smaller than the diameter of the SiO_2 nanoparticles. The top $(PSS/AChE)_3$ sensing film cannot fully cover the nanoparticles and smoothen the surface. However, it can "passivate" the nanoparticles and provide a protection coat for the device. Fig. 2(d) shows the cross-sectional image of the assembled thin film, which consists of a SWNT multilayer and a SiO_2 nanoparticle multilayer. The SWNTs and SiO_2 nanoparticles are closely packed in the film.

The ISFET sensor was characterized using an HP 4156A semiconductor parameter analyzer. During the measurement, the ISFET was partially dipped in the ACh solution (volume of 500 μl). The channel area was completely immersed in the solution and the elongated electrode pads remained exposed in the air. The source electrode was connected to ground (GND) and the drain electrode was applied with an external voltage V_D. The Ag/AgCl probe, used as the gate reference electrode, was also immersed in the ACh solution and approximately 5 mm away from the channel. The probe was applied with a gate voltage V_G. All the measurements were done at room temperature.

3. Results and discussion

The SWNT is first measured for the functionality, i.e., the field-effect, in a 10 mM ACh solution. The output characteristics of the SWNT ISFET are shown in Fig. 3(a). The device shows an explicit field effect and typical p-type transistor characteristics. The gate and drain voltages V_G and V_D are negative; V_G is swept from −2 to 0 V with a 0.4 V step and V_D is swept from 0 to −1 V with a −20 mV step. A higher $|V_G|$ results in a higher drain current $|I_D|$. The gate transfer characteristics of the same device are shown in Fig. 3(b). V_D is fixed at −1 V and V_G is swept from 0 to −2 V with a −10 mV step. The threshold voltage $V_{TH} = -0.25$ V is obtained from the figure by linearly extrapolating the gate transfer curve to the x-axis. Based on the traditional MOSFET theory [19], the hole mobility of the SWNT ISFET in the saturation region is calculated as $\mu_p = 80.32\ cm^2/Vs$.

However, a leakage current from the semiconducting layer to the gate reference electrode is observed for the ISFET sensor, as shown in Fig. 4. One important reason for this current to occur is the formation of the dielectric film, which consists of PDDA and SiO_2 nanoparticles. In the solution, the PDDA polyelectrolytes expand and induce charge transfer within the dielectric film. The holes in the semiconducting channel can move inside the dielectric film and then to the electrode through the expanded polyelectrolytes. The leakage current is one of the major differences between our self-assembled nanotube/nanoparticle ISFET sensor and the conventional Si-based devices. It brings uncertainties to the device performance and its influences should be eliminated for sensor calibration. Further investigation will be conducted to solve the problem. One potential solution to reduce the leakage current is to use plasma-enhanced chemical vapor deposition (PECVD) instead of the LbL self-assembly in dielectric layer deposition. The PECVD technique can grow a dense and highly insulating SiO_2 film; however, it increases the fabrication cost at the same time.

After verifying the field-effect functionality, the SWNT ISFET is measured for its sensing ability towards ACh. The device is immersed in ACh solutions with various concentrations and the drain current I_D is recorded by the semiconductor analyzer. V_G is set as −2 V so that the device operates in the saturation region. V_D

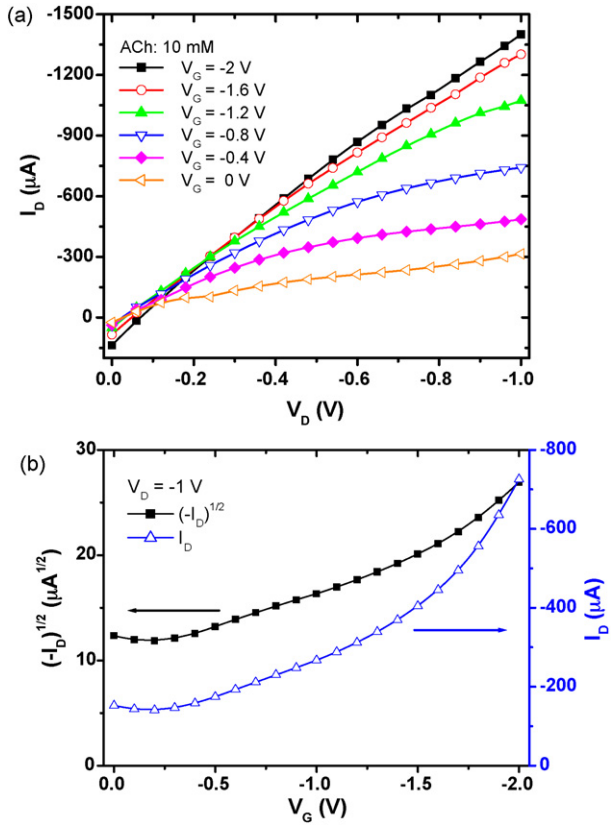

Fig. 3. (a) Drain current-voltage characteristics of an SWNT ISFET in a 10 mM ACh solution. (b) Gate characteristics of the same device at the saturation region.

is scanned from 0 to −1 V with a −10 mV step. Fig. 5 shows the recorded drain current at various ACh concentrations. At higher concentrations from 10 μM to 10 mM, the differences between the curves are distinct. However, at lower concentrations from 1 pM to 1 μM, the curves are very close and hard to be distinguished from one another. Therefore, the currents at $V_D = -1$ V and $V_G = -2$ V are extracted from Fig. 5 and plotted as a function of the ACh concentration in Fig. 6(a). The main figure demonstrates the response of the ISFET sensor over the full ACh concentration range. The curve stays relatively flat in the low concentration range up to 1 μM. At

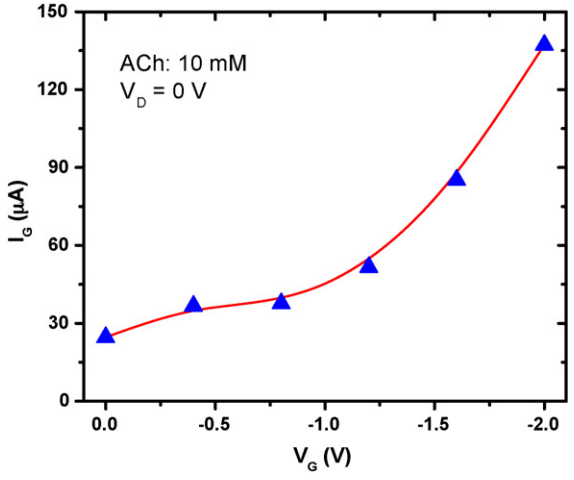

Fig. 4. Gate leakage current with respect to gate voltage. Drain voltage V_D is fixed at 0 V.

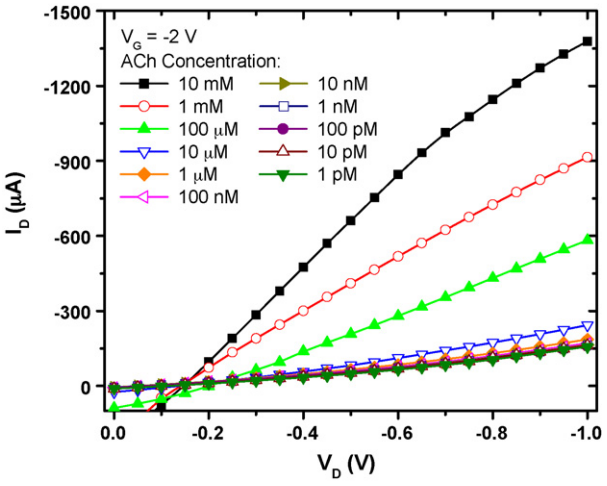

Fig. 5. Drain current-voltage curves of an SWNT ISFET in different ACh solutions.

higher concentrations, from 10 μM to 10 mM, a dramatic increase is observed and the curve within this range is linear. The sensitivity of this sensor equals to the slope of the linear region and it is measured as 378.2 μA/decade. Compared with the SWNT thin-film ACh sensor (sensitivity: 7.2 μA/decade) [13], the sensitivity of the ISFET sensor

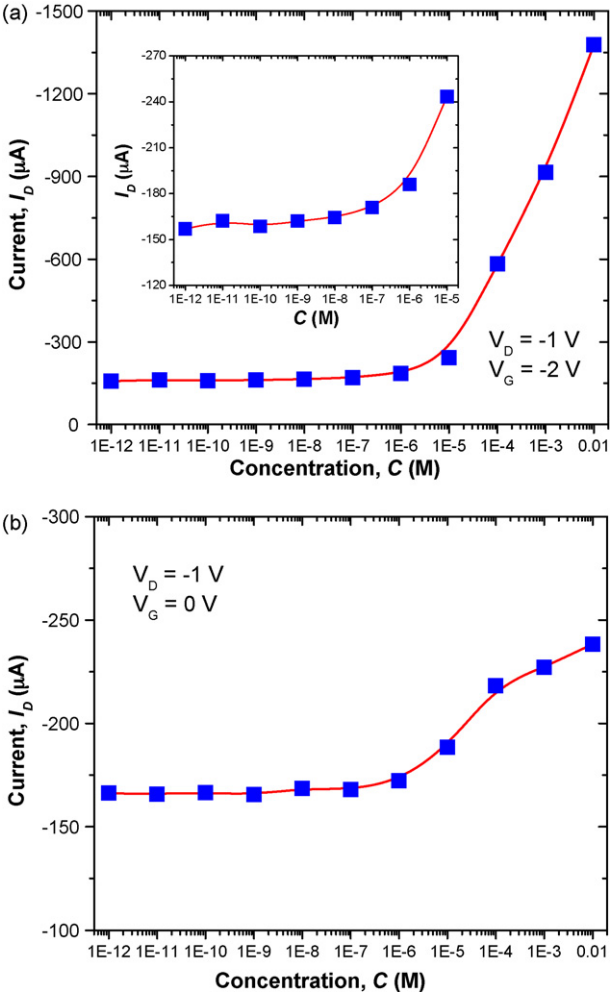

Fig. 6. ACh response of an SWNT ISFET with (a) $V_G = -2$ V and (b) $V_G = 0$ V. $V_D = -1$ V for both curves.

is 52.53 times higher. Although the current-concentration curve in the low ACh range appears flat, the magnified view shows a slight current increase, as shown in the inset of Fig. 6(a). In the range of 1 pM–1 nM, the current is approximately 160 μA with neglectable variations. When the ACh concentration is increased from 10 nM to 10 μM, the current shows a nonlinear increase. Therefore, the resolution of the ISFET sensor is determined to be 10 nM. Compared with the previously developed In_2O_3 nanoparticle ACh sensor (resolution: 100 nM; sensitivity: 12.4 μA/decade) [15], the SWNT ISFET sensor shows higher performance in terms of both resolution and sensitivity. Because the two devices have similar structures and identical dielectric layers, it is likely the performance is primarily determined by the semiconducting material. However, when compared with the SWNT thin-film ACh sensor (resolution: 100 pM, linear range: 100 pM–10 mM) [13], the ISFET sensor shows reduced resolution and linearity. Further research is in progress in order to increase the device resolution while maintaining its high sensitivity.

Fig. 6(b) illustrates the current change of the same device when it is applied with a different gate voltage $V_G = 0$ V. The current remains relatively constant at lower ACh concentrations up to 100 nM and then increases at higher concentrations from 1 μM to 10 mM. The sensitivity of the device in the high concentration range is approximately 16.6 μA/decade. Compared with the device at $V_G = -2$ V (resolution: 10 nM; sensitivity: 378.2 μA/decade), the performance of the device at $V_G = 0$ V is much lower. The linearity of the characteristic curve is also decreased. Therefore, the gate voltage V_G has high influences on the performance of the ISFET ACh sensor.

When the device is exposed to ACh, the released hydrogen ions from the ACh hydrolysis add a bias voltage V_B between the gate and source electrodes. The actual gate voltage applied on the ISFET is therefore changed by V_B. If there is no other external voltage applied on the reference electrode, the gate voltage equals to the bias voltage. The hydrolysis of ACh determines the magnitude and changing rate of V_B. Therefore, the response time of the device can be estimated by measuring the bias voltage. Fig. 7(a) shows the real-time response of an ISFET to ACh solution recorded by a data acquisition system. The measurement starts by immersing the device in 500 μl deionized water. ACh solutions with various concentrations (500 μl for each concentration) are injected to the bulk solution using a pipette. The voltage remains relatively constant when 1 nM and 1 μM ACh solutions are injected. However, when 1 mM and 10 mM ACh solutions are injected, the voltage increases dramatically. An expanded view of the voltage response is shown in Fig. 7(b). When the 1 mM ACh solution is injected at the 480th sec, the voltage shows a small decrease first and a sharp increase afterwards. The decrease is caused by the manual injection of the solution and the increase is caused by the released hydrogen ions from the enzymatic reaction. The bias voltage reaches a steady state in 15 s and is approximately 17 mV. However, due to the concentration difference between the injected solution and the bulk solution, the hydrogen ions continue to diffuse until the bulk solution reaches an equilibrium condition. Therefore, a continuous decrease of the voltage is observed.

Compared with the SWNT thin-film sensor (response time: 6 s) [13], the ISFET has a longer response time. The difference is mainly caused by the diffusion distance of the hydrogen ions. For the thin-film sensor, the hydrogen ions penetrate inside the SWNT film and change its conductance. The diffusion time is limited by the thickness of the surface AChE sensing layer. The diffusion distance of the hydrogen ions is only in the range of 30 nm. However, for the ISFET sensor, the hydrogen ions diffuse to the bulk solution until a steady state is reached between the AChE sensing layer and the gate reference electrode. The diffusion distance is in the range of

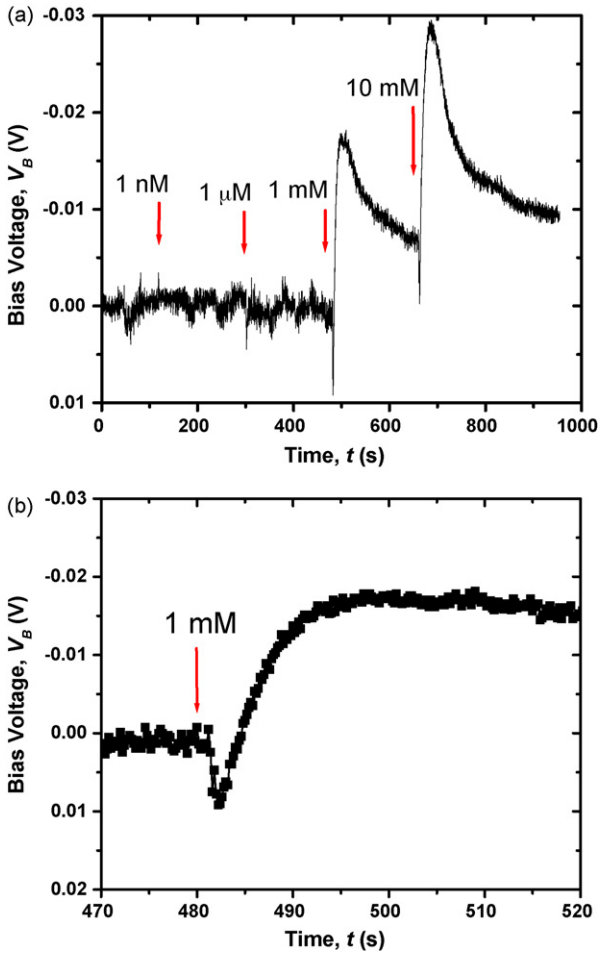

Fig. 7. (a) Response time measurement of an SWNT ISFET. (b) A magnified view of the response curve when the 1 mM ACh solution is injected.

5 mm, which is much longer than that of the thin-film sensor. It is possible that the response time of the ISFET can be reduced by moving the Ag/AgCl probe closer to the sensing layer or integrating the gate electrode on the same substrate. In the latter case, the diffusion distance can be dramatically shortened to several micrometers.

To study the long-term stability, the sensor is characterized in a 10 mM ACh solution; the operational conditions are $V_G = -2$ V and $V_D = -1$ V for all the measurements. The sensor is first submerged in the ACh solution and the current is recorded by the HP 4156A analyzer. Next, it is naturally dried and stored in air at room temperature. The device is measured again under the same condition after 24 h. The measurement procedure is repeated for 9 consecutive days, as shown in Fig. 8. The device shows noticeable current changes after 3 days. The average current is recorded as −1.27 mA and the standard deviation is 0.11 mA. The long-term stability of this device is relatively lower than most Si-based ISFET sensors. The main reason is that the active components of the sensor are composite films. Even though the SWNTs and SiO_2 nanoparticles are immobilized on the device and held together by the PDDA electrostatic "glue", they are not as robust as the bulk Si and SiO_2. During the measurement, especially in the soaking and drying cycles, the assembled materials may slightly change their positions and directions. One possible method to solve the problem is to grow more densely assembled nanomaterial films on the device. Another solution is to coat an additional film on the surface to

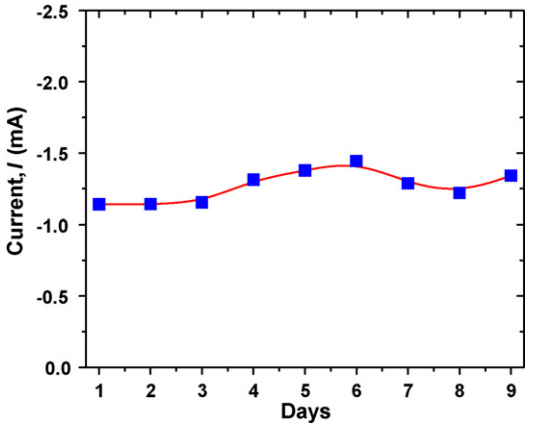

Fig. 8. Stability of the SWNT thin-film transistor in a 10 mM ACh solution. $V_G = -2$ V and $V_D = -1$ V.

protect the nanomaterials. These methods can reduce the material motion in different environments and enhance the stability of the sensor.

Several groups have investigated the ISFET technology in ACh sensing applications. For example, I. Willner et al reported an enzyme monolayer-functionalized FET as an ACh sensor [9]. The sensitivity, resolution, and response time of the sensor are 44.2 mV/decade, 10 μM, and 30 s, respectively. S.-K. Hsiung et al reported an extended gate FET to detect ACh [20]. The device shows a sensitivity of 28 mV/decade in the concentration range of 1–2.5 mM. Most of these reported sensors are Si-based transistors with immobilized AChE monolayers as the sensing components. Compared with these devices, our sensor uses various nanomaterials as the active components. The Si wafer is only used as a support. The sensor shows relative higher or comparable performance in many key parameters. Although the nanomaterial-based ISFET is still in the early stage of the development, our study shows that it is a promising technique and shows high potential in sensing applications. As a matter of fact, a number of researchers have already participated in the investigation of ISFET technology using nanomaterials [21]. We expect that the performance of these nanomaterial-based ISFET sensors can be dramatically increased in the near future.

4. Conclusion

We have successfully developed a high-sensitivity and low-cost ACh sensor using the SWNT thin-film transistor as a platform. The SWNTs, SiO_2 nanoparticles, and AChE enzyme molecules are deposited on the device as the semiconducting, dielectric, and sensing layers, respectively. The transistor is highly sensitive to the concentration change of hydrogen ions due to the ACh hydrolysis reaction. The gate voltage dramatically enhances the drain current and the sensitivity of the sensor. The characterization shows that the ISFET is a promising technique for ACh sensing. The performance of the ISFET sensor can be further enhanced by optimizing the design parameters such as channel dimensions and the number of self-assembled layers. In addition, with the corresponding enzymes assembled on the surface, the ISFET can be used as a platform for sensing many types of biomolecules.

Acknowledgements

We thank Prof. Stephen A. Campbell at the Department of Electrical and Computer Engineering at the University of Minnesota for using his laboratory for the electrical characterization. We thank the staff members in the Nanofabrication Center and the Characterization Facility at the University of Minnesota for their help with the experimental work. This work is partially supported by the Defense Advanced Research Projects Agency (DARPA) MEMS/NEMS Fundamental Research Program through the Micro/Nano Fluidic Fundamentals Focus (MF3) Center.

References

[1] B. Liu, Y.-H. Yang, Z.-Y. Wu, H. Wang, G.-L. Shen, R.-Q. Yu, A potentiometric acetylcholinesterase biosensor based on plasma-polymerized film, Sens. Actuators B 104 (2005) 186–190.
[2] S. Lin, C.-C. Liu, T.-C. Chou, Amperometric acetylcholine sensor catalyzed by nickel anode electrode, Biosens. Bioelectron. 20 (2004) 9–14.
[3] P. Uutela, R. Reinilä, P. Piepponen, R.A. Ketola, R. Kostiainen, Analysis of acetylcholine and choline in microdialysis samples by liquid chromatography tandem mass spectrometry, Rapid Commun. Mass Sp. 19 (2005) 2950–2956.
[4] R. Dunphy, D.J. Burinsky, Detection of choline and acetylcholine in a pharmaceutical preparation using high-performance liquid chromatography/electrospray ionization mass spectrometry, J. Pharm. Biomed. Anal. 31 (2003) 905–915.
[5] A.G. Hadd, S.C. Jacobson, J.M. Ramsey, Microfluidic assays of acetylcholinesterase inhibitors, Anal. Chem. 71 (1999) 5206–5212.
[6] A. Riklin, I. Willner, Glucose and acetylcholine sensing multilayer enzyme electrodes of controlled enzyme layer thickness, Anal. Chem. 67 (1995) 4118–4126.
[7] G.-P. Jin, X.-Q. Lin, J.-M. Gong, Novel choline and acetylcholine modified glassy carbon electrodes for simultaneous determination of dopamine, serotonin and ascorbic acid, J. Electroanal. Chem. 569 (2004) 135–142.
[8] S. Godoy, B. Leca-Bouvier, P. Boullanger, L.J. Blum, A.P. Girard-Egrot, Electrochemiluminescent detection of acetylcholine using acetylcholinesterase immobilized in a biomimetic Langmuir-Blodgett nanostructure, Sens. Actuators B 107 (2005) 82–87.
[9] A.B. Kharitonov, M. Zayats, A. Lichtenstein, E. Katz, I. Willner, Enzyme monolayer-functionalized field-effect transistors for biosensor applications, Sensor. Actuators B 70 (2000) 222–231.
[10] Y. Miao, J. Guan, J. Chen, Ion sensitive field effect transducer-based biosensors, Biotechnol. Adv. 21 (2003) 527–534.
[11] P. Bergveld, Thirty years of ISFETOLOGY: what happened in the past 30 years and what may happen in the next 30 years, Sensor. Actuators B 88 (2003) 1–20.
[12] F. Patolsky, C.M. Lieber, Nanowire nanosensors, Mater. Today 8 (2005) 20–28.
[13] W. Xue, T. Cui, A high-resolution amperometric acetylcholine sensor based on nano-assembled carbon nanotube and acetylcholinesterase thin film, J. Nano R. 1 (2008) 1–9.
[14] Y. Liu, A.G. Erdman, T. Cui, Acetylcholine biosensors based on layer-by-layer self-assembled polymer nanoparticle ion-sensitive field-effect transistors, Sensor. Actuators A 136 (2007) 540–545.
[15] Y. Liu, T. Cui, Nano self-assembled nanoparticle ion-sensitive field-effect transistors for acetylcholine biosensing, in: 2nd IEEE International Conference on Nano/Micro Engineered and Molecular Systems, Bangkok, Thailand, January 16–19, 2007, pp. 382–385.
[16] W. Xue, T. Cui, Carbon nanotube micropatterns and cantilever arrays fabricated with layer-by-layer nano self-assembly, Sensor. Actuators A 136 (2007) 510–517.
[17] W. Xue, Y. Liu, T. Cui, High-mobility transistors based on nanoassembled carbon nanotube semiconducting layer and SiO_2 nanoparticle dielectric layer, Appl. Phys. Lett. 89 (2006) 163512.
[18] W. Xue, T. Cui, Characterization of layer-by-layer self-assembled carbon nanotube multilayer thin films, Nanotechnology 18 (2007) 145709.
[19] B.G. Streetman, S. Banerjee, Solid State Electronic Devices, 6th ed., Prentice Hall, Englewood Cliffs, NJ, 2005.
[20] L.-L. Chi, L.-T. Yin, J.-C. Chou, W.-Y. Chung, T.-P. Sun, K.-P. Hsiung, S.-K. Hsiung, Study on separative structure of EnFET to detect acetylcholine, Sensor. Actuators B 71 (2000) 68–72.
[21] X.-L. Luo, J.-J. Xu, W. Zhao, H.-Y. Chen, A novel glucose ENFET based on the special reactivity of MnO_2 nanoparticles, Biosens. Bioelectron. 19 (2004) 1295–1300.

Biographies

Wei Xue received the BS and the MS degrees in electrical engineering from Shandong University, Jinan, China, in 1997 and 2000, respectively, and the PhD degree in mechanical engineering from the University of Minnesota, Minneapolis, MN, in 2007. He is currently an assistant professor of mechanical engineering at Washington State University, Vancouver. Before he joined WSU, he was a postdoctoral research associate at the Department of Mechanical Engineering, University of Minnesota. His main research interest includes microfabrication techniques, nanotechnology, polymer/silicon microelectromechanical systems (MEMS), micro/nano electronics, and chemical/biological sensors.

Tianhong Cui received the BS degree from Nanjing University of Aeronautics and Astronautics in 1991, and the PhD degree from the Chinese Academy of Sciences in

1995. He is currently a Nelson associate professor of mechanical engineering at the University of Minnesota. From 1999 to 2003, he was an assistant professor of electrical engineering at Louisiana Technical University. Prior to that, he was a STA fellow at National Laboratory of Metrology, and served as a postdoctoral research associate at the University of Minnesota and Tsinghua University. He received research awards including the Nelson Endowed Chair Professorship from the University of Minnesota, the Research Foundation Award from Louisiana Tech University, the Alexander von Humboldt Award in Germany, and the STA & NEDO fellowships in Japan. He is a senior member of IEEE and a member of ASME. His current research interests include MEMS/NEMS, nanotechnology, and polymer electronics.